Received: 7 June 2022 | Revised: 27 July 2022 | Accepted: 2 August 2022

DOI: 10.1002/jmor.21502

RESEARCH ARTICLE

JOURNAL OF morphology WILEY

Three-dimensional fine structure of fibroblasts and other mesodermally derived tissues in the dermis of adults of the Bahamas lancelet (Chordata, Cephalohordata), as seen by serial block-face scanning electron microscopy

Nicholas D. Holland[1] | Linda Z. Holland[1] | Ildiko M. L. Somorjai[2]

[1]Marine Biology Research Division, Scripps Institution of Oceanography, University of California at San Diego, La Jolla, California, USA

[2]School of Biology, University of Saint Andrews, St. Andrews, Fife, Scotland, UK

Correspondence
Nicholas D. Holland, Marine Biology Research Division, Scripps Institution of Oceanography, University of California at San Diego, La Jolla, CA 92093, USA.
Email: nholland@ucsd.edu

Funding information
Welcome trust ISSF#; NSF grant IOS 1952567

Abstract

Tissues of adult cephalochordates include sparsely distributed fibroblasts. Previous work on these cells has left unsettled such questions as their developmental origin, range of functions, and even their overall shape. Here, we describe fibroblasts of a cephalochordate, the Bahamas lancelet, *Asymmetron lucayanum*, by serial block-face scanning electron microscopy to demonstrate their three-dimensional (3D) distribution and fine structure in a 0.56-mm length of the tail. The technique reveals in detail their position, abundance, and morphology. In the region studied, we found only 20 fibroblasts, well separated from one another. Each was strikingly stellate with long cytoplasmic processes rather similar to those of a vertebrate telocyte, a possibly fortuitous resemblance that is considered in the discussion section. In the cephalochordate dermis, the fibroblasts were never linked with one another, although they occasionally formed close associations of unknown significance with other cell types. The fibroblasts, in spite of their name, showed no signs of directly synthesizing fibrillar collagen. Instead, they appeared to be involved in the production of nonfibrous components of the extracellular matrix—both by the release of coarsely granular dense material and by secretion of more finely granular material by the local breakdown of their cytoplasmic processes. For context, the 3D structures of two other mesoderm-derived tissues (the midline mesoderm and the posteriormost somite) are also described for the region studied.

KEYWORDS

amphioxus, extracellular matrix, midline mesoderm, posteriormost segment, telocyte

1 | INTRODUCTION

Within the phylum Chordata, lancelets or amphioxus (members of subphylum Cephalochordata) are widely considered to provide the best available insight into the features of the proximate invertebrate ancestor of the subphylum Vertebrata. This point of view has been fortified in recent years by results from molecular phylogeny (Delsuc et al., 2008) and genomics (Yue et al., 2014). This presumed key phylogenetic position of cephalochordates has long stimulated studies of their biology (Holland & Holland, 2017). Unfortunately, the degree of coverage has varied markedly across life history stages and from one tissue to the next. For instance, the wealth of information on developmental genetics for embryos and early larvae has not yet been matched by comparable studies on later larvae, metamorphic animals, and adults. Similarly, even at the level of cell and tissue morphology of adult cephalochordates, some features have been inadequately studied. One such feature is the fibroblast, the focus of the present investigation.

Previous work has shown that the cephalochordate fibroblast is a relatively rare cell type that has never been detected before the late larval stages (Mansfield et al., 2015). Moreover, its cytodifferentiative origin is unknown (Stach, 2000). Finally, there is not even wide agreement about the overall cell shape. Early cytologists, observing squash preparations, reported that cephalochordate fibroblasts had a stellate outline, whereas, more recent histologists, studying sectioned tissue, reached the current consensus that the cells have a relatively compact overall shape.

Here, we take a fresh look at cephalochordate fibroblasts with a recently developed (and still developing) technique: namely, serial block-face scanning electron microscopy (SBSEM). With this method, cells can be reconstructed in three dimensions (3D) and related in fine detail to neighboring structures (Kornfield & Denk, 2018). The innovative feature of SBSEM is the inclusion of an ultramicrotome in the specimen chamber of the microscope. Initially, the SEM scans the face of the specimen block, and the backscattered signal is expressed as an image superficially resembling a transmission electron micrograph (TEM). Then, the microtome shaves away a thin layer of the block surface to expose a new block face for the next scan. The regular alternation of scanning and shaving generates a series of images that can be converted to 3D by computer programs.

All of the earlier work on cephalochordate fibroblasts was done on species in the relatively accessible genus *Branchiostoma*. Here, in contrast, we describe the distribution and fine structural topography of fibroblasts in *Asymmetron lucayanum*, the Bahamas lancelet, a genus characterized by an extremely thin posterior caudal process (cp in Figure 1a) rich in cell types yet low in overall tissue volume. This facilitates 3D reconstructions of the fine structure by SBSEM. For the same tissue volume, previous publications by Holland and Somorjai (2020a, 2020b) have provided context for the present study by describing the extracellular materials of the dermal matrix, the notochord, and the peripheral sensory nerves plus related glia. In the present study, to examine all possible heterocellular associations between fibroblasts and neighboring cells, we include descriptions of two additional mesodermally derived tissues—first, the midline mesoderm (already known for *Branchiostoma*) and, second, the posteriormost somite (not known before in cephalochordates).

This is an opportune time for a study of cephalochordate fibroblasts due to the current upsurge in interest in suggesting homologies at the level of cell types across appreciable distances in the tree of life (Sachkova & Burkhardt, 2019). New techniques like single-cell transcriptomics have raised the possibility that their application to lancelet fibroblasts might show whether such cells are innovations or the evolutionary source of the diverse subpopulations of fibroblasts known to characterize vertebrates (Buechler et al., 2021).

2 | MATERIALS AND METHODS

For SBSEM studies, we collected adult specimens of *A. lucayanum*, each 1.8 cm long, from the soft substratum at low tide in the Bimini lagoon (25.72297° N, 79.29288° W), North Bimini Island, Bahamas, in October 2019. An approximately 2-mm length of tail was cut from

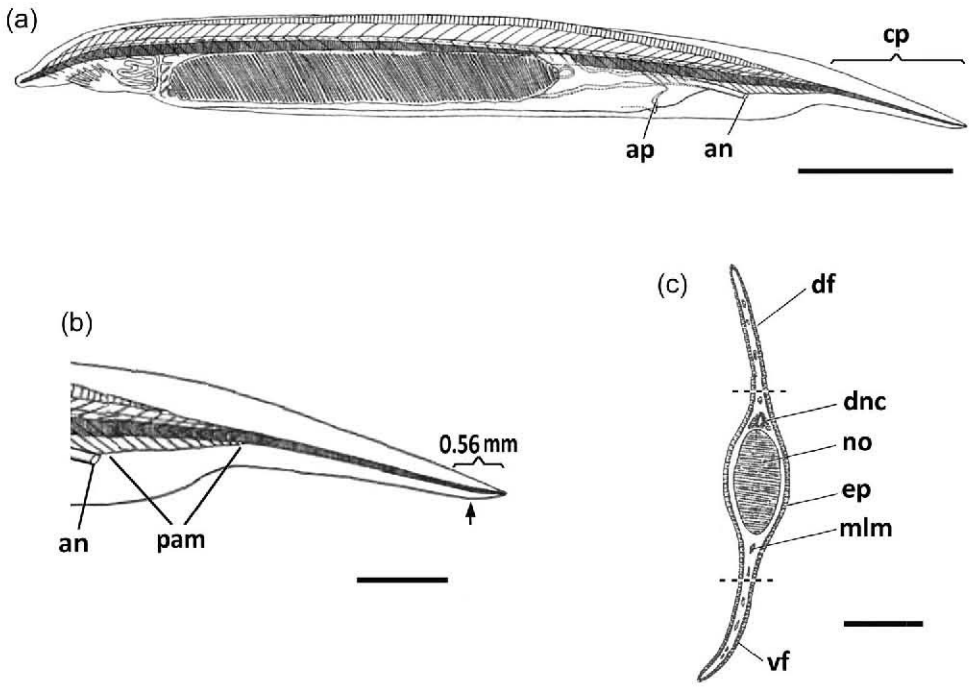

FIGURE 1 *Asymmetron lucayanum*, Bahamas lancelet (all from Andrews, 1893). (a) Adult in left-side view. Scale bar, 3 mm. (b) Tail region posterior to the anus (an) with postanal myomeres (pam) indicated. The bracket shows the 0.56-mm length of the caudal process sampled by SBSEM. Scale bar, 1 mm. (c) Cross-section of the caudal process (at arrow in panel b). Scale bar, 25 μm. ap, atriopore; cp, caudal process; df, dorsal fin; dnc, dorsal nerve cord; ep, epidermis; mlm, midline mesoderm; no, notochord; SBSEM, serial block-face scanning electron microscopy; vf, ventral fin.

the posterior end and placed in the primary fixative (0.15 mol l^{-1} cacodylate buffer [pH 7.4] containing 2% formaldehyde, 1.5% glutaraldehyde, and 2 mmol l^{-1} $CaCl_2$) at 4°C for 2 weeks (Deerinck et al., 2010). The postfixation sequence was: reduced osmium tetroxide, thiocarbohydrazide, osmium tetroxide, uranyl acetate, and lead aspartate as detailed in Wanner et al. (2016). After dehydration in ethanol, specimens were transferred through acetone and embedded in Durcupan resin.

For SBSEM, the block faces were scanned in a 3View system (Gatan) in a Zeiss Merlin SEM. After each block face was imaged by a scanning electron microscope, a microtome in the specimen chamber shaved away a 0.25-µm-thick layer of the block, exposing a new surface. Alternation of scanning and shaving generated uninterrupted serial images looking superficially like conventional TEM. We oriented tissue blocks to obtain cross-sections starting at the tail tip and cut the most favorably oriented specimen. In all, 2240 consecutive block faces were imaged (covering an anterior–posterior distance of 560 µm). As emphasized by the bracketed region in Figure 1b, this is a modest amount of tissue (representing only about 0.1% of the volume of the whole animal). Moreover, the field of view of the studied region was not large enough to include the edges of the dorsal and ventral fins (df and vf in Figure 1c). Even so, the tissue volume we studied was *quite large* in the context of most other SBSEM studies to date.

The serial, two-dimensional SBSEM images were converted to 3D with the *Reconstruct* Program available gratis from http://www.bu.edu/neural/Reconstruct.html (Borrett & Hughes, 2016; Fiala, 2005). The 3D structures were visualized as Boissonnat surfaces. For views down short segments of the anterior–posterior axis of the tail, more limited reconstructions were made from 60 consecutive SBSEM sections (equivalent to a 15-µm-thick, semitransparent steak seen in cross-section). Similarly, from the tail of another animal, serial frontal sections were made to afford a 3D view in the dorsal–ventral axis of the body. To create a terminology for cell types applicable to cephalochordates generally, instead of one adapted to a single genus, we include some highlights from our unpublished SBSEM study of the tail tip of a 1.8-cm-long young adult of a second cephalochordate genus and species (*Branchiostoma floridae*) from a laboratory culture maintained at Scripps Institution of Oceanography (Holland & Li, 2021).

3 | RESULTS

3.1 | Fibroblasts

Table 1 reviews the various names applied to cephalochordate fibroblasts (all from the genus *Branchiostoma*) and shows how a consensus to use the term "fibroblast" eventually emerged. The present SBSEM study demonstrated that, like *Branchiostoma*, *Asymmetron* has fibroblasts; those of the latter genus were too few to have been noticed previously by light microscopists (Andrews, 1893; Holland & Somorjai, 2021). In the present study, we found fibroblasts were relatively rare—only 20 of them were detected in the reconstructed region (Figure 2a,b). They were widely separated from one another and showed no obvious patterns of distribution in the dorsoventral or mediolateral axes of the body (Figure 2c,d).

Each fibroblast comprised a central nuclear region from which extend long cytoplasmic processes (from two to five) that tended to branch and rebranch along their course. These processes (Figure 2e, tandem arrow; Figure 3a, arrow) often ran close to the inner surface of the collagen fibril layer (cfl) but were never observed to penetrate deeper into its substance. The cell extensions of the fibroblast (Figure 2e) are often moniliform (i.e., small-diameter regions alternate with dilations). In the dermal matrix, just outside the plasma membrane of each fibroblast, were some extracellular vesicles (Figure 2e, arrowheads) as defined by Witwer & Théry (2019). In their moniliform processes and associated extracellular vesicles, the fibroblasts resemble vertebrate telocytes, a circumstance that will be examined in Section 4.1 of our discussion.

Within the fibroblast cytoplasm are a few mitochondria and some vesicles up to 0.5 µm in diameter with low-density contents. Also present are irregularly shaped dense masses up to a few micrometers in diameter (Figure 2e, single arrow). The largest of these tend to be located in the perinuclear cytoplasm, while the smaller ones occur within the cytoplasm of the cell processes. These masses are composed of tightly aggregated granules, each roughly 200 nm in diameter. Such dense masses have no counterpart in a vertebrate fibroblast (or in a vertebrate telocyte). It is possible that they are destined to be released to form some of the predominantly granular material in the dermal matrix (whether this might include precursors of fibrillar collagens is not known). In a few places, small packets of cytoplasm are found in isolation (shown in a broad context at the tandem arrows in Figure 2a,b). Each packet, as seen in SBSEM images, is filled with dense granular material (inset in Figure 2e, arrowheads), evidently blebbed off from the rest of the fibroblast. This might represent a route for the secretion of dense material into the extracellular matrix.

TABLE 1 Names (some anglicized) used for fibroblast in previous studies of *Branchiostoma*

Name	Reference(s)
Star-shaped cell	Langerhans (1876), Owsjannikow (1868), and Schneider (1879)
Connective tissue cell	Metchnikoff (1892)
Spindle cell	Schneider (1902)
Network cell	Goldschmidt (1908)
Fibrocyte	Olsson (1961)
Fibroblast-like cell	Mansfield et al. (2015)
Fibroblast	Ruppert (1997), Stach (2000), and Welsch (1968)

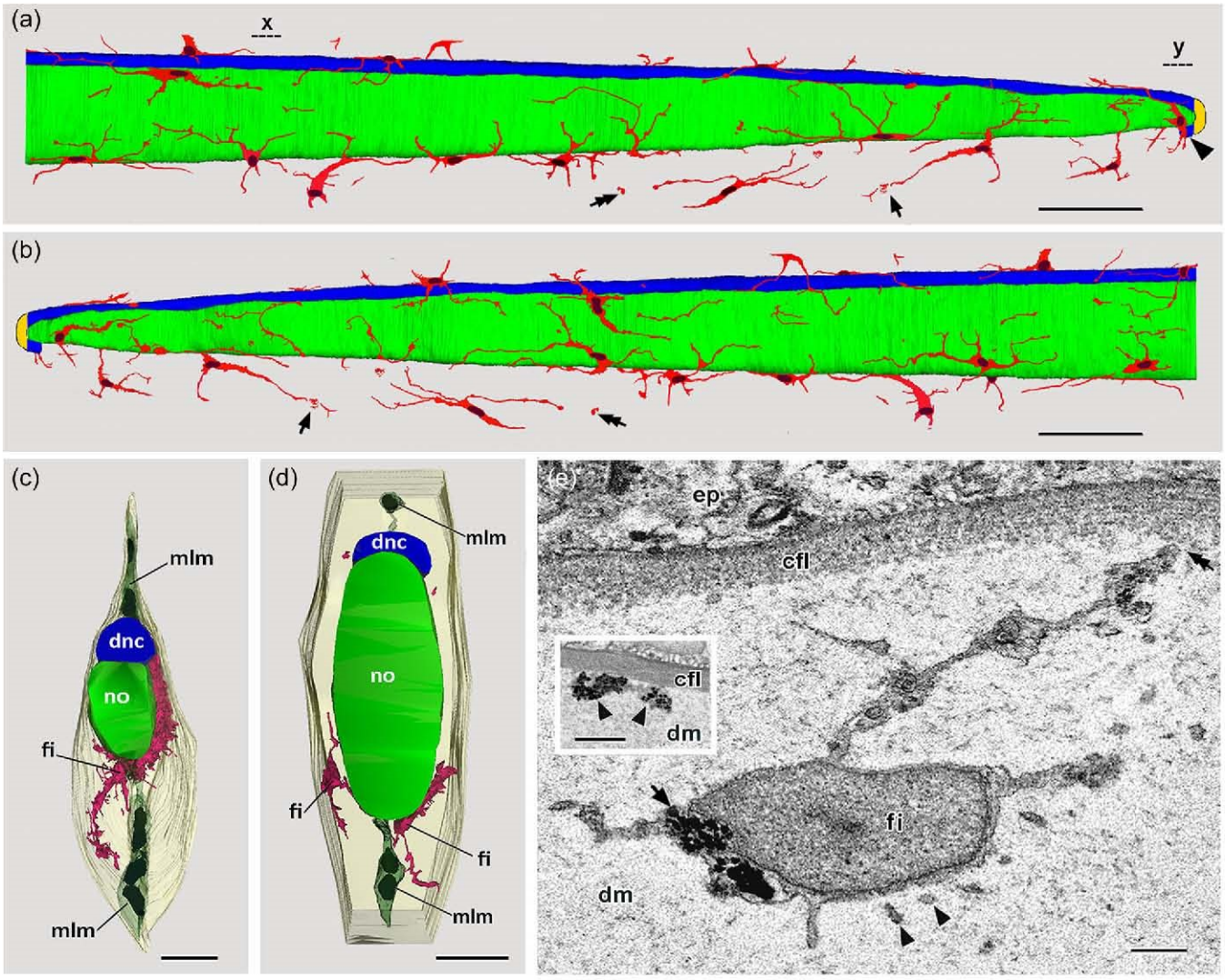

FIGURE 2 *Asymmetron lucayanum*. (a) Fibroblasts (red) in studied region of caudal process in left-side view. The posterior extremity of the dorsal nerve cord (blue) curls ventrally around the notochord (green) and terminates at the arrowhead; the yellow zone shows where a few dorsal nerve cord cells were cut away during block trimming. Arrow indicates the cell region shown in SBSEM in Figure 4a. A tandem arrow indicates a small isolated packet of cytoplasm. Scale bar, 50 µm. (b) Same as panel a, but the right-side view. Arrow indicates the cell region shown in SBSEM in Figure 4a. A tandem arrow indicates a small isolated packet of cytoplasm. Scale bar, 50 µm. (c) Cross-section of 15-µm-thick reconstruction (seen from anterior, along dashed line y in panel a). A fibroblast (fi) is red; notochord (no) is dark green, dorsal nerve cord (dnc) is blue, and midline mesoderm (mlm) is light green. Scale bar, 10 µm. (d) Like panel c, but along dashed line x in panel a. Scale bar, 10 µm. (e) SBSEM image of the nuclear region of fibroblast (fi) in the dermal matrix (dm) extending a moniliform process with three dilations; the distal region of the process (tandem arrow) runs close to the inner surface of the collagen fibril layer (cfl). Arrowheads indicate extracellular vesicles; a single arrow indicates dense cytoplasmic mass. Scale bar, 1 µm. Inset shows cytoplasmic bleb, presumably from fibroblast, containing dense material (arrowheads). Inset scale bar, 2 µm. SBSEM, serial block-face scanning electron microscopy.

Another peculiarity of *Asymmetron* fibroblasts is the tendency of parts of their cytoplasmic processes to rupture and release cytoplasmic material (evidently differing from the dense inclusions already mentioned) into the surrounding extracellular matrix of the dermis. An instance of such breakage in progress is shown in a broad context in Figure 2a,b (single arrows) where a short, dilated region of a process appears to have burst. Figure 4a is an SBSEM image showing this location in detail: plasma membrane fragments (arrowheads) from the burst process surround a zone of finely granular material (asterisk). The latter might represent the addition of components to the dermal matrix (again, whether some of this is a precursor for fibrillar collagens is not known).

Cell–cell associations between neighboring fibroblasts in *Asymmetron* were never detected. However, the fibroblasts occasionally formed close heterocellular associations. Thus, the nuclear region and/or cytoplasmic processes of the fibroblasts may be juxtaposed to the following: posteriormost somite cells (Figure 3a, arrowhead), glial cells of sensory peripheral nerves (Figure 3b), notochord (Figure 3c, arrow), dorsal nerve cord (Figure 3d, arrowhead), or cells of the midline mesoderm (Figure 3d, arrow).

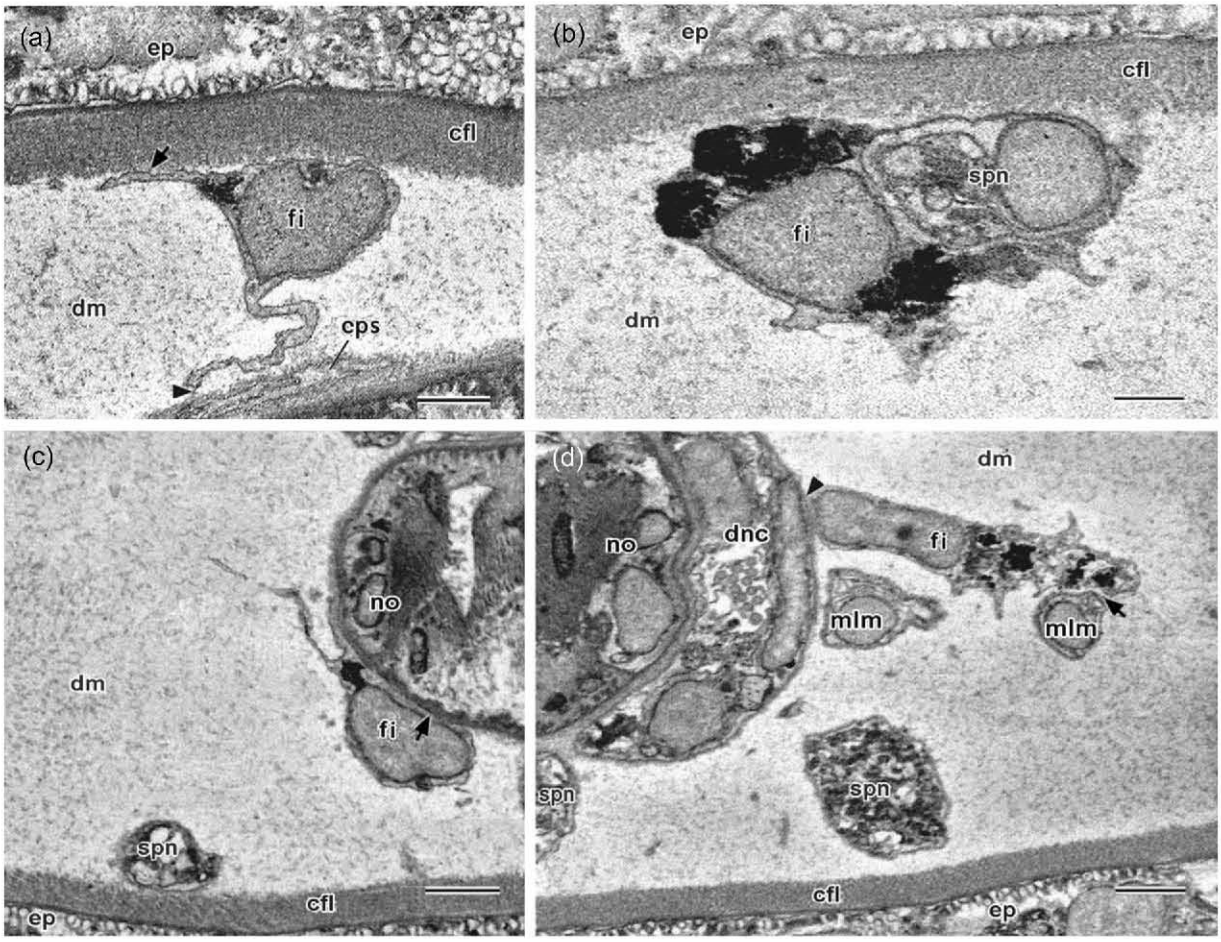

FIGURE 3 *Asymmetron lucayanum*. (a) SBSEM image of fibroblast (fi) contacting collagen fibril layer (cfl) at arrow and associated with the cell of posteriormost somite (cps) at arrowhead. Scale bar, 1 µm. (b) SBSEM image of fibroblast closely associated with glial cell of sensory peripheral nerve. Scale bar, 1 µm. (c) Fibroblast is closely associated with the notochord (arrow). Scale bar, 2 µm. (d) Fibroblast associated both with dorsal nerve cord (arrowhead) and cell of midline mesoderm (arrow). Scale bar, 2 µm. dm, dermal matrix; dnc, dorsal nerve cord; ep, epidermis; mlm, midline mesoderm; no, notochord; SBSEM, serial block-face scanning electron microscopy; spn, sensory peripheral nerve.

No clear associations were found between any parts of the fibroblasts and the collagenous microligaments (terminology of Ruppert, 1997), which are then strands of fibrillar collagen arising perpendicularly from the collagen fibril layer (Figure 4b). In some places, microligaments appeared to run all the way across the body, inserting at either end of the collagen fibril layer (Figure 4c,d). Somewhat disconcertingly, in contrast to what we observed in *Asymmetron*, Olsson (1961) and Ruppert (1997) reported close associations between the fibroblasts and some of the microligaments in *Branchiostoma*.

3.2 | Midline mesoderm cells

The midline mesoderm cells were once misunderstood to be parts of blood vessels (Marcusen, 1864) or lymph spaces (Andrews, 1893). However, in recent years, they have come to be considered as a tissue unique to cephalochordates (Ruppert, 1997). In the region sampled, there were 125 nuclei belonging to this cell type (Figure 5a,b), each presumably indicating an individual cell, although cell boundaries were not detectable. Some of these cells (Figure 5c) were located along the edges of the dorsal and ventral fins, but most were distributed in interconnected strands running through the dermal matrix close to the mid-sagittal plane of the body, as best demonstrated in cross-sections (Figure 2c,d). The cytoplasm of the midline mesoderm cells included a few mitochondria, secretory granules, and rough endoplasmic reticulum containing granular material (Figure 5d). The clear release of this granular material into the extracellular compartment was not directly observed, although such exocytosis likely produces a substantial fraction of the proteinaceous components of the dermal matrix.

3.3 | Posteriormost somite tissue

An adult cephalochordate has a series of chevron-shaped muscular segments running along either side of the entire body. Ruppert (1997, p. 388) discusses the complicated usage of synonyms (namely,

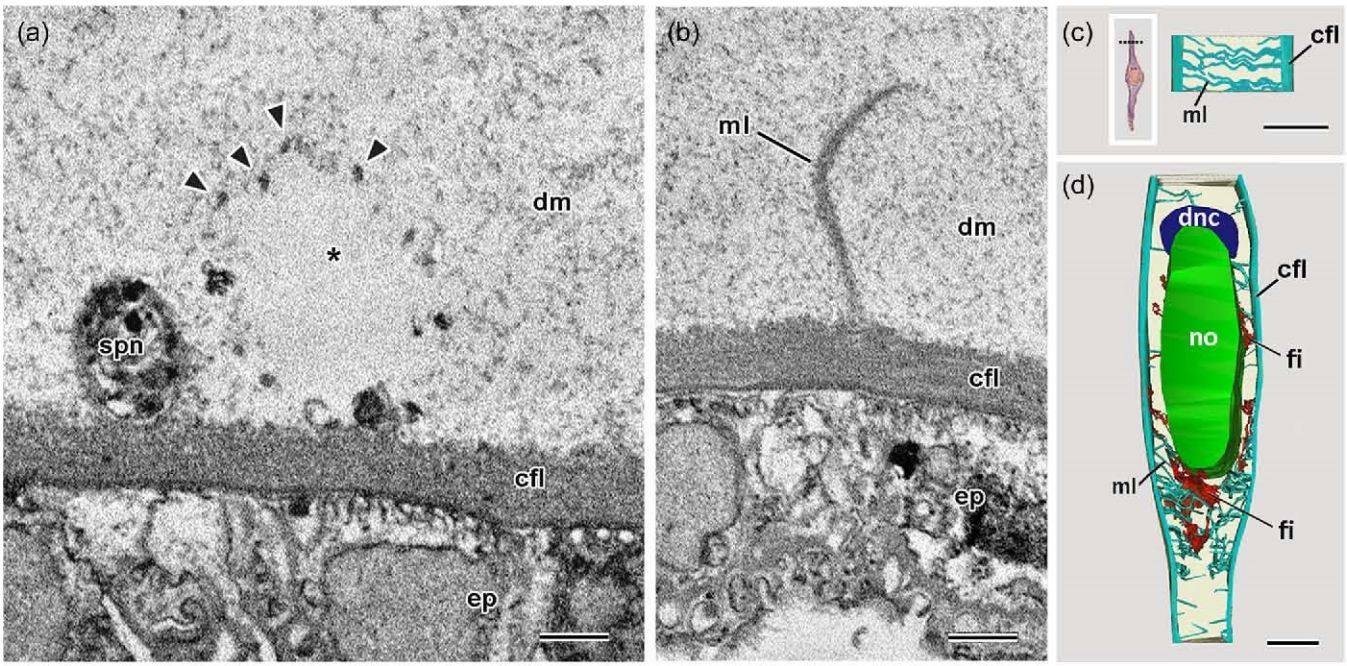

FIGURE 4 *Asymmetron lucayanum*. (a) SBSEM image of arrowed cell region in Figure 2a,b, showing possible secretion of the finely granular dermal matrix (asterisk) externalized by a bursting cytoplasmic process of a fibroblast; arrowheads indicate small vesicles evidently derived from the fibroblast plasma membrane. Scale bar, 1 µm. (b) SBSEM image of collagenous microligament (ml) extending from collagen fibril layer (cfl) into dermal matrix (dm). Scale bar, 1 µm. (c) Frontal section through microligaments (ml) and collagen fibril layers (both turquoise) at the level of dotted line in the inset. Scale bar, 5 µm. (d) A 15-µm-thick reconstruction of body cross-section (epidermis omitted); microligaments (ml) arise from collagen fibril layer (cfl) (both turquoise). Scale bar, 10 µm. dm, dermal matrix; dnc, dorsal nerve cord; ep, epidermis; fi, fibroblast; no, notochord; SBSEM, serial block-face scanning electron microscopy; spn, sensory peripheral nerve.

somites, myotomes, and myomeres) for such cephalochordate segments. Here, we use his definition of a *myomere* as comprising both the medial muscular wall plus the lateral, nonmuscular wall of each segment. In cephalochordates generally, the maximum number of myomeres is reached around the time of larval metamorphosis and then remains stable for the rest of the life history (Schubert et al., 2001). In addition, we here coin a new term, "posteriormost somite," for some previously overlooked mesoderm forming an inconspicuous, nonmuscular serial homolog of the muscular myomere series. In *Asymmetron*, this tissue (Figure 6a,b) comprises irregularly shaped plaques of cells interconnected by cytoplasmic strands and associated with the left, ventral, and right surface of the notochord. In the region sampled, 242 nuclei were present, presumably representing individual cells.

The more posterior plaques were one-cell thick (Figure 6c), while the more anterior ones (Figure 6d) were organized into flattened sacs with an apical and a basal cell layer separated by a small lumen. The cytoplasm included a few mitochondria as well as small vesicles and granules up to about 1 µm in diameter; however, no endoplasmic reticulum was detected. The posteriormost somite tissue is never separated from the notochord by an underlying cell sac (i.e., the mesothelium surrounding the sclerocoel) of the sort always accompanying each muscular myomere. For *Asymmetron*, we prefer to consider all the plaques associated with the surface of the notochord to represent a simple, poorly organized epithelium. In *Branchiostoma* (our unpublished observation), the comparable tissue is organized into a single, discreet epithelial sac on either side of the posterior tip of the notochord. Importantly, the fibroblasts in this posterior region of *Branchiostoma* (our unpublished data), like those of *Asymmetron*, are widely scattered and stellate, showing that these features are cephalochordate-specific and not specializations associated with the unusual caudal process of the latter genus.

The anterior-to-posterior development of myomeres along the developing cephalochordate body has been described previously for cephalochordates only in the genus *Branchiostoma* (Schubert et al., 2001). Briefly, during the stage of the neurula embryo, the first 10 or so myomeres evaginate from the dorsolateral mesendoderm of the body wall, without the participation of a posterior tail bud. Subsequently, during the early- to mid-larval stages, several dozen more myomeres arise from a tail bud (namely, by budding off from the lateral walls of the neurenteric canal). Finally, in late larvae, approximately 10 more myomeres are progressively added posterior to the anus in some unknown way; perplexingly, the postanal myomeres are posterior to any endoderm, so a complete tail bud with a neurenteric canal would no longer be present. The posteriormost somite presumably appears during or just after the formation of the postanal myomeres and evidently endures for the rest of their life history; however, until postanal myomere development is understood, nothing definite can be said about the first beginnings of the posteriormost somite.

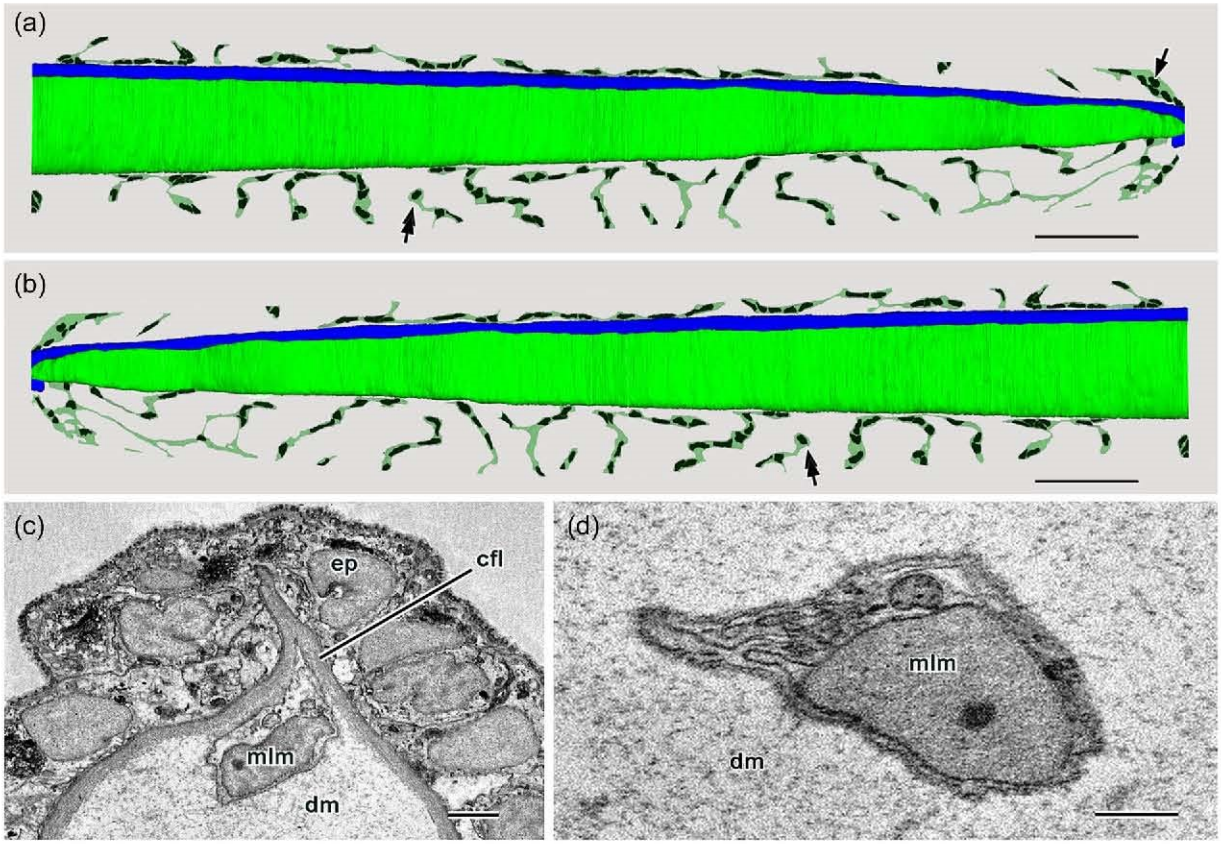

FIGURE 5 *Asymmetron lucayanum*. (a) Midline mesoderm cells in studied region of caudal process in left-side view with black nuclei in light green cytoplasm without indication of cell boundaries and epidermis is not shown. The notochord is dark green and the nerve cord is blue. Scale bar, 50 μm. (b) Like foregoing, but in right-side view. Scale bar, 50 μm. (c) Serial block-face scanning electron microscopy (SBSEM) image of cross-section, showing dermal matrix (dm) surrounding midline mesoderm cell (mlm) located at single arrow in (a) and associated with collagen fibril layer (cfl) just beneath epidermis (ep). Scale bar, 2 μm. (d) SBSEM image of dermal matrix (dm) surrounding midline mesoderm cell (mlm) at the position indicated by tandem arrows in (a and b). Scale bar, 2 μm.

4 | DISCUSSION

4.1 | Cephalochordate fibroblasts versus vertebrate telocytes

As mentioned in Section 3.1, there are some interesting parallels between *Asymmetron* fibroblasts and vertebrate telocytes (Kondo & Kaestner, 2019; Manole & Simionescu, 2016; Vannucchi, 2020). For example, in telocyte terms, each entire moniliform cytoplasmic process in Figure 2e would be called a *telopode*, and its alternating thin regions and dilations would, respectively, be called *podomeres* and *podons*. Moreover, *Asymmetron* fibroblasts are often associated with extracellular vesicles (Figure 2e, arrowheads), which are highly characteristic of telocytes (as described by Fertig et al., 2015). In spite of the foregoing similarities, however, we do not think the broader evidence (summarized in Table 2) indicates a homologous relationship between cephalochordate fibroblasts and vertebrate telocytes, especially the lack of fibroblast-to-fibroblast association. The fibroblasts thus contrast markedly with vertebrate telocytes, which typically associate with each other via homocellular junctions to form a network with no strong tendency to fragment (Rosa et al., 2021).

4.2 | Functions and possible homologies of cephalochordate fibroblasts

In the present study, we found no clear evidence (like the presence of fibripositors, mentioned below) to suggest that *Asymmetron* fibroblasts are involved in the eponymous function of directly synthesizing collagen fibrils. Discordantly, however, a TEM observation on *Branchiostoma* fibroblasts (Welsch, 1968) clearly showed one such cell with internal fibripositors, which Kadler (2017) described as typical of vertebrate fibroblasts producing nascent collagen fibrils. In addition, Mansfield et al. (2015) illustrated the nuclear region of a fibroblast (although without fibripositors) deeply embedded within the collagen fibril layer of an adult *Branchiostoma*.

The present study of *Asymmetron* fibroblasts found no clear signs of collagen fibril synthesis but did suggest that such cells synthesize and release granular components of the extracellular matrix of the dermis. Additional sources of the granular extracellular matrix are likely the midline mesoderm cells with their conspicuously distended cisternae of the endoplasmic reticulum. In the future, the whole spectrum of dermal matrix components should be thoroughly characterized at the molecular level. The results of such studies

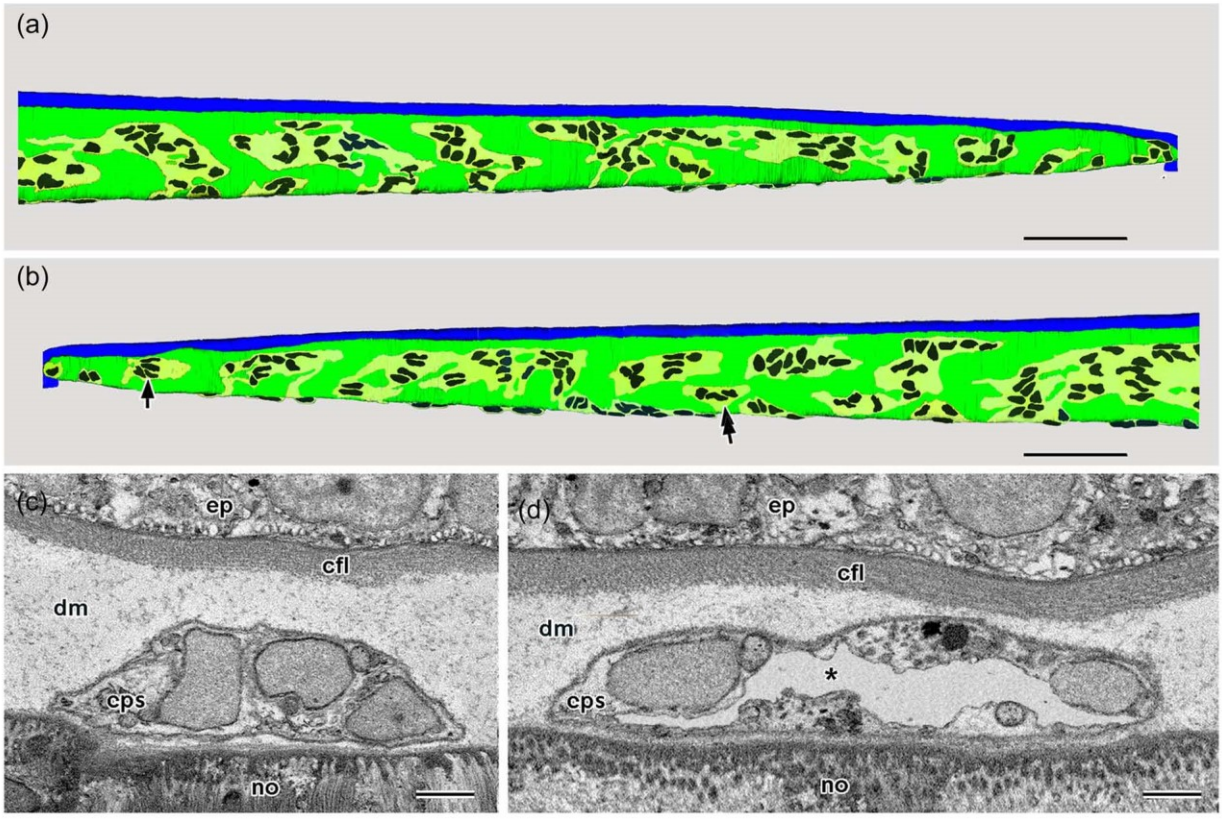

FIGURE 6 *Asymmetron lucayanum*. (a) Cells of posteriormost somite in studied region of caudal process in left-side view. These cells, which are associated with the surface of the notochord, are shown with black nuclei in yellow cytoplasm, but cell boundaries are not indicated, and the epidermis is not shown. The notochord is green and the dorsal nerve cord is blue. Scale bar, 50 µm. (b) Like foregoing, but right-side view. Scale bar, 50 µm. (c, d) These SBSEM images are frontal views (i.e., at right angles to panels a and b); so top to bottom is lateral to medial. In (c), the cells of the posteriormost somite (at single arrow in panel b) are not arranged around a lumen; in contrast, in (d), such cells (at tandem arrow in panel b) surround a narrow lumen (asterisk). Scale bars, 2 µm. ep, epidermis; cfl, collagen fibril layer; dm, dermal matrix; cps, cells of the posteriormost somite; no, notochord; SBSEM, serial block-face scanning electron microscopy.

TABLE 2 Comparing vertebrate telocytes and cephalochordate fibroblasts

Feature	Vertebrate telocyte	*Asymmetron* fibroblast	*Branchiostoma* fibroblast (unpublished)
Location	Mostly organ stroma[a]	Dermis[b]	Dermis[b,c]
Shape stellate	Yes	Yes	Yes
Processes moniliform	Yes	Yes	No
Processes fragment	No	Yes	Yes
Extracellular vesicles	Yes	Yes	No
Homocellular junctions	Yes	No	No
Heterocellular junctions	Yes	Yes	Yes
Large dense inclusions	No	Yes	No

[a]Vertebrate telocytes occur mostly in the stroma of solid organs and only rarely in the dermis (Manole & Simionescu, 2016); cephalochordate organs have no stroma (Hatschek, 1888).

[b]Cells located in each myoseptum have been considered fibroblasts by Mansfield et al. (2015), although Rähr (1979) considered them to be part of the circulatory system and not part of the dermis; further study will be needed to resolve this problem.

[c]Dermal fibroblasts are illustrated by Ruppert (1997, p. 374) as abundant just beneath the collagen fibril layer (however, these might have been confounded with midline mesoderm cells).

should be especially interesting because it is likely that these dermal matrix components in cephalochordates represent a stage in chordate connective tissue evolution destined to favor mineralization, thus setting the stage for the evolution of vertebrate skeletons, as discussed by Yong and Yu (2017).

It remains possible that the uniform-looking fibroblasts in the cephalochordate dermis may be hiding heterogeneity at transcriptomic and other levels of organization, as is now realized for vertebrate fibroblasts (Atit et al., 2018; Plikus & Krieg, 2021). In other words, one might reasonably suggest that cephalochordate fibroblasts, notwithstanding their apparent morphological uniformity, could have given rise to the recently appreciated plethora of fibroblast subtypes in vertebrates (Buechler et al., 2021). Should that be so, chordate fibroblasts would be particularly relevant for addressing the question of cell-type evolution during the origin of the vertebrates.

5 | CONCLUSIONS

SBSEM can do more than simply add exquisite new details to what is already known. First, the technique can correct serious misconceptions (here, e.g., fibroblast shape in cephalochordates is shown not to be compact, but strikingly stellate); second, it can bring to light entirely new tissues (here, e.g., the posteriormost somites in the myomere series), and third, it can point the way to further work on previously demonstrated but poorly studied structures like the postanal myomeres. Even more usefully, SBSEM data can lead to new hypotheses and experimental approaches for relating cell structure and function. For instance, a promising avenue of research suggested by the present study would be to apply single-cell transcriptomics to cephalochordate fibroblasts to uncover possible functional diversity hidden by seeming morphological uniformity. Such studies could lead to interesting new proposals for cell-type homologies across major taxa.

AUTHOR CONTRIBUTIONS

Nicholas H. Holland: Conceptualization; funding acquisition; data curation; 3D reconstructions; writing original draft; editing. **Ildiko M. L. Somorjai:** Conceptualization; funding acquisition; collection and culture of *Asymmetron lucayanum*; data curation; writing review; editing. **Linda Z. Holland:** Conceptualization; funding acquisition; data curation; laboratory maintenance of breeding colony of *Branchiostoma floridae* at Scripps Institution of Oceanography; writing review; editing.

ACKNOWLEDGMENTS

Personnel at the Bimini Field Station (Sharklab) helped us collect *Asymmetron*. Jennifer Santini and Marcella Erb of the UCSD School of Medicine Microscopy Core assisted with SBSEM. The SBSEM facility and staff support are funded by the UCSD School of Medicine Microscopy Core Grant P30 NS047101. *Branchiostoma* research at Scripps Institution of Oceanography is supported by NSF Grant IOS 1952567 to Linda Z. Holland and Nicholas H. Holland. Research in the Somorjai lab is funded by Welcome Trust ISSF# and EU Horizon 2020 grants INFRADRVA (654248) and INFEA Assemble (930984). We also thank Gregory Rouse for making photocopies of three figures in Andrews (1893).

CONFLICT OF INTEREST

The authors declare no conflict of interest.

DATA AVAILABILITY STATEMENT

Data are available on request from the authors.

ORCID

Nicholas D. Holland http://orcid.org/0000-0002-3448-490X
Linda Z. Holland http://orcid.org/0000-0003-2960-9437
Ildiko M. L. Somorjai http://orcid.org/0000-0001-5243-6664

REFERENCES

Andrews, E. A. (1893). An undescribed acraniate: *Asymmetron lucayanum*. *Studies from the Biological Laboratory Johns Hopkins University*, *5*, 213–247.

Atit, R., Thulabandu, V., & Chen, D. M. (2018). Dermal fibroblast in cutaneous development and healing. *Wiley Interdisciplinary Reviews in Developmental Biology*, *7*, article e307.

Borrett, S., & Hughes, L. (2016). Reporting methods for processing and analysis of data from serial block face scanning electron microscopy. *Journal of Microscopy*, *263*, 3–9.

Buechler, M. B., Pradhan, R. N., Krishnamurty, A. T., Cox, C., Calviello, A. K., Wang, A. W., Yang, Y. A., Tam, L., Caothien, R., Roose-Grima, M., Modrusan, Z., Arron, J. R., Bourgon, R., Müller, S., & Turley, S. J. (2021). Cross-tissue organization of the fibroblast lineage. *Nature*, *593*, 575–579.

Deerinck, T. J., Bushong, E. A., Lev-Ram, Y., Shu, X., Tsien, R. Y., & Elisman, M. H. (2010). Enhancing serial block-face scanning electron microscopy to enable high resolution 3-D nanohistology of cells and tissues. *Microscopy & Microanalysis*, *16*, 1138–1139.

Delsuc, F., Tsagkogeorga, G., Lartillot, N., & Philippe, H. (2008). Additional molecular support for the new chordate phylogeny. *Genesis*, *46*, 592–604.

Fertig, E. T., Gherghiceanu, M., & Popescu, L. M. (2015). Extracellular vesicles release by cardiac telocytes: Electron microscopy and electron tomography. *Journal of Cellular & Molecular Medicine*, *18*, 1938–1943.

Fiala, J. C. (2005). *Reconstruct*: A free editor for serial section microscopy. *Journal of Microscopy*, *218*, 52-61.

Goldschmidt, R. B. (1908). Die Bindegewebe des Amphioxus. *Sitzungsberichte der Gesellschaft für Morphologie und Physiologie in München*, *24*, 53–78.

Hatschek, B. (1888). Über den Schichtenbau von Amphioxus. *Anatomischer Anzeiger*, *3*, 662–667.

Holland, L. Z., & Li, G. (2021). Laboratory culture and mutagenesis of amphioxus (*Branchiostoma floridae*). *Methods in Molecular Biology*, *2219*, 1–29.

Holland, N. D., & Holland, L. Z. (2017). The ups and downs of amphioxus biology: A history. *International Journal of Developmental Biology*, *61*, 575–583.

Holland, N. D., & Somorjai, I. M. L. (2020a). The sensory peripheral nervous system in the tail of a cephalochordate studied by serial blockface scanning electron microscopy. *Journal of Comparative Neurology*, *528*, 2569–2582.

Holland, N. D., & Somorjai, I. M. L. (2020b). Serial blockface SEM suggests that stem cells may participate in adult notochord growth in an invertebrate chordate, the Bahamas lancelet. *EvoDevo*, *10*, article 11.

Holland, N. D., & Somorjai, I. M. L. (2021). Tail regeneration in a cephalochordate, the Bahamas lancelet, *Asymmetron lucayanum*. *Journal of Morphology*, *282*, 217–229.

Kadler, K. E. (2017). Fell Muir Lecture: Collagen fibril formation in vitro and in vivo. *International Journal of Experimental Pathology*, *98*, 4–16.

Kondo, A., & Kaestner, K. H. (2019). Emerging diverse roles of telocytes. *Development*, *146*, article 175018.

Kornfield, J., & Denk, W. (2018). Progress and remaining challenges in high-throughput volume electron microscopy. *Current Opinion in Neurobiology*, *50*, 261–267.

Langerhans, P. (1876). Zur Anatomie des *Amphioxus lanceolatus*. *Archiv für Mikroskopische Anatomie*, *12*, 290–348.

Manole, C. G., & Simionescu, O. (2016). The cutaneous telocytes. In S. D. Wang, & D. Cretoiu (Eds.), *Telocytes, connecting cells* (pp. 303–322). Springer.

Mansfield, J. H., Haller, E., Holland, N. D., & Brent, A. E. (2015). Development of somites and their derivatives in amphioxus, and implications for evolution of vertebrate somites. *EvoDevo*, *6*, article 21.

Marcusen, M. J. (1864). Sur l'anatomie et l'histologie du *Branchiostoma lubricum*, Costa (*Amphioxus lanceolatus*, Yarrell). Seconde note. *Comptes Rendues Hebdomadaires des Séances de l'Académie des Sciences*, *59*, 89–90.

Metchnikoff, E. (1892). *Leçons sur la Pathologie Comparée de l'Inflammation: Faites à l'Institut Pasteur en Avril et Mai 1891* (p. 239). Masson.

Olsson, R. (1961). The skin of amphioxus. *Zeitschrift für Zellforschung und Mikroskopische Anatomie*, *54*, 90–104.

Owsjannikow, P. (1868). Über das Centralnervensystem des *Amphioxus lanceolatus*. *Bulletin de l'Académie Impériale des Sciences de St.-Pétersbourg*, *12*, 287–302.

Plikus, M. V., & Krieg, T. (2021). More than just bricks and mortar: Fibroblasts and ECM in skin health and disease. *Experimental Dermatology*, *30*, 4–9.

Rähr, H. (1979). The circulatory system of amphioxus [*Branchiostoma lanceolatum* (Pallas)]. A light microscopic investigation based on intravascular injection technique. *Acta Zoologica Stockholm*, *60*, 1–18.

Rosa, I., Marini, M., & Manetti, M. (2021). Telocytes: An emerging component of stem cell niche microenvironment. *Journal of Histochemistry & Cytochemistry*, *69*, 795–818.

Ruppert, E. E. (1997). Cephalochordata (Acrania). In F. W. Harrison, & E. E. Ruppert (Eds.), *Microscopic anatomy of invertebrates, Volume 15, Hemichordata, Chaetognatha, and the invertebrate chordates* (pp. 349–504). Wiley-Liss.

Sachkova, M., & Burkhardt, P. (2019). Exciting times to study the identity and evolution of cell types. *Development*, *146*, article 178996.

Schneider, A. (1879). Beiträge zur vergleichenden Anatomie und Entwicklungsgeschichte der Wirbelthiere. I. *Amphioxus lanceolatus* (p. 31). Reimer.

Schneider, K. (1902). *Lehrbuch der vergleichenden Histologie der Tiere* (p. 988). Fischer.

Schubert, M., Holland, L. Z., Stokes, M. D., & Holland, N. D. (2001). Three amphioxus *Wnt* genes (*AmphiWnt3*, *AmphiWnt5*, and *AmphiWnt6*) are associated with the tail bud: The evolution of somitogenesis in chordates. *Developmental Biology*, *240*, 262–272.

Stach, T. (2000). Microscopic anatomy of developmental stages of *Branchiostoma lanceolatum* (Cephalochordata, Chordata). *Bonner Zoologische Monographien*, *47*, 1–111.

Vannucchi, M. G. (2020). The telocytes: Ten years after their introduction in the scientific literature. An update on their morphology, distribution, and potential roles in the gut. *International Journal of Molecular Sciences*, *21*, article 4478.

Wanner, A. A., Genoud, C., & Friedrich, R. W. (2016). 3-dimensional electron microscopic imaging of the zebrafish olfactory bulb and dense reconstruction of neurons. *Scientific Data*, *3*, article 160100.

Welsch, U. (1968). Beobachtungen über die Feinstruktur der Haut und des äusseren Atrialepithels von *Branchiostoma lanceolatum* Pall. *Zeitschrift für Zellforschung*, *88*, 565–575.

Witwer, K. W., & Théry, C. (2019). Extracellular vesicles of exosomes. On primacy, precision, and popularity influencing a choice of nomenclature. *Journal of Extracellular Vesicles*, *8*, article 1648167.

Yong, L. W., & Yu, J. K. (2017). Tracing the evolutionary origin of vertebrate skeletal tissues: Insights from cephalochordate amphioxus. *Current Opinion in Genetics & Development*, *39*, 55–62.

Yue, J. X., Yu, J. K., Putnam, N. H., & Holland, L. Z. (2014). The transcriptome of an amphioxus, *Asymmetron lucayanum*, from the Bahamas, a window into chordate evolution. *Genome Biology & Evolution*, *6*, 2681–2696.

How to cite this article: Holland, N. D., Holland, L. Z., & Somorjai, I. M. L. (2022). Three-dimensional fine structure of fibroblasts and other mesodermally derived tissues in the dermis of adults of the Bahamas lancelet (Chordata, Cephalohordata), as seen by serial block-face scanning electron microscopy. *Journal of Morphology*, *283*, 1289–1298. https://doi.org/10.1002/jmor.21502